Journal Pre-proof

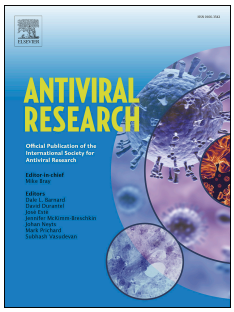

Artemisinin inhibits the replication of flaviviruses by promoting the type I interferon production

Xugang Wang, Bohan Zheng, Usama Ashraf, Hao Zhang, Chen Cao, Qi Li, Zheng Chen, Muhammad Imran, Huanchun Chen, Shengbo Cao, Jing Ye

PII: S0166-3542(20)30224-2

DOI: https://doi.org/10.1016/j.antiviral.2020.104810

Reference: AVR 104810

To appear in: *Antiviral Research*

Received Date: 3 December 2019

Revised Date: 28 February 2020

Accepted Date: 25 April 2020

Please cite this article as: Wang, X., Zheng, B., Ashraf, U., Zhang, H., Cao, C., Li, Q., Chen, Z., Imran, M., Chen, H., Cao, S., Ye, J., Artemisinin inhibits the replication of flaviviruses by promoting the type I interferon production, *Antiviral Research*, https://doi.org/10.1016/j.antiviral.2020.104810.

Artemisinin inhibits the replication of flaviviruses by promoting the type I interferon production

Xugang Wang[1,2,3], Bohan Zheng[1,2,3], Usama Ashraf[1,2], Hao Zhang[1,2,3], Chen Cao[1,2,3], Qi Li[1,2,3], Zheng Chen[1,2,3], Muhammad Imran[1,2,3,] Huanchun Chen[1,2,3], Shengbo Cao[1,2,3], Jing Ye[1,2,3*]

Affiliations:

[1]State Key Laboratory of Agricultural Microbiology, Huazhong Agricultural University, Wuhan, Hubei, 430070, PR China

[2]Laboratory of Animal Virology, College of Veterinary Medicine, Huazhong Agricultural University, Wuhan, Hubei, 430070, PR China

[3]The Cooperative Innovation Center for Sustainable Pig Production, Huazhong Agricultural University, Wuhan, Hubei, 430070, P. R. China

* Corresponding authors.

E-mail addresses: yej@mail.hzau.edu.cn (Jing Ye)

Abstract

Flaviviruses are considered to be major emerging human pathogens globally. Currently available anti-flavivirus approaches are ineffective, thus there is a desperate need for broad-spectrum drugs that can be active against existing and emerging flaviviruses. Artemisinin has been found to cause an antiviral effect against several viruses; however, its antiviral effect against flaviviruses remains unexplored. Here the antiviral activity of artemisinin against flaviviruses such as JEV, DENV, and ZIKV was evaluated by measuring the hallmark features of virus replication both *in vitro* and *in vivo*. Mechanistically, the artemisinin-induced antiviral effect was associated with enhanced host type I interferon response. The blocking of interferon signaling inhibited the artemisinin-induced interferon-stimulated genes expression and rescued the artemisinin-suppressed virus replication. This study demonstrated for the first time the antiviral activity of artemisinin against flaviviruses with a novel antiviral mechanism. The therapeutic application of artemisinin may constitute a broad-spectrum approach to cure infections caused by flaviviruses.

KEYWORDS: artemisinin; flavivirus; antiviral; therapy; type I interferon

1. Introduction

The genus Flavivirus, belonging to the *Flaviviridae* family, comprises many important pathogens that pose a serious threat to the human population annually (Bradley et al., 2017; Carlo et al., 2014). Some flaviviruses, such as Japanese encephalitis virus (JEV) and West Nile virus (WNV), have the potential to infect the host central nervous system (CNS), deemed as neurotropic viruses (E A Gould, 2008; Gregorius et al., 2012). In addition, Zika virus (ZIKV) has recently become a public health concern due to its association with microcephaly in infants and Guillain-Barré syndrome (GBS) in adults (Capasso et al., 2019; Hirsch et al., 2018). Dengue virus (DENV), a causative agent of dengue fever and dengue shock syndrome, also exhibits a potential of being a neurotropic virus (Amorim et al., 2019; Calderón-Peláez et al., 2019).

The pathogenesis of flaviviruses is complex and primarily classified into three distinct phases that include initial infection, viremia, and severe symptoms (Ye et al., 2013). Initial infection and viremia are associated with the replication of viruses in dendritic cells and macrophages (Diamond, 2003; Imran et al., 2019). Then, the host may exhibit various clinical symptoms and even death (Chen et al., 2018). Some flaviviruses such as JEV and WNV breach the blood-brain barrier, and subsequently infect the CNS wherein they trigger the host inflammatory response (Maximova et al., 2018; Mustafá et al., 2019) characterized by gliosis, rampant production of inflammatory cytokines, and eventually neuronal cell damage (Ashraf et al., 2016; Zhang et al., 2015). The interplay between flavivirus pathogenicity and the host innate and adaptive immune responses governs the neuropathogenesis and resultant effect of the flavivirus infection (Ngono et al., 2018; Olagnier et al., 2016).

Natural products serve as beneficial chemical scaffolds for the development of effective therapeutics (Wohlfarth et al., 2009). Artemisinin, for instance, is not only known to be active

against malaria, but also to other diseases, including cancer (Wong et al., 2017) and some fungal (Denny et al., 2019), parasitic (Idowu et al., 2018), and viral (Efferth et al., 2008) infections. Several studies provided strong evidence for the antiviral activity of artemisinin and its synthetic analogues against herpesviruses, hepatitis C virus, and human immunodeficiency virus, whereas the pieces of evidence are weaker for papillomaviruses and polyomaviruses (Efferth, 2018; Sharma et al., 2014). However, their mechanisms of antiviral activity are largely unknown. Despite all these research progresses, the antiviral roles of artemisinin and its derivatives against flaviviruses have not yet been investigated. At present, there are no distinct antiviral therapies available to treat patients suffering from infections caused by flaviviruses (Boldescu et al., 2017). Consequently, the quest for active and safe antiviral agents showing a broad-spectrum activity against emerging and life-threatening flaviviruses is urgently needed. Herein, we demonstrated the antiviral activity of artemisinin against flaviviruses such as JEV, ZIKV, and DENV. Treatment with artemisinin reduced mortality and ameliorated JEV-mediated brain damage in a mouse model. The observed anti-flaviviral activity of artemisinin was associated with an enhanced host IFN-I response. These data suggest a broad-spectrum therapeutic potential of artemisinin against flaviviruses.

2. Methods

2.1 Cell cultures and viruses

Adenocarcinomic human alveolar epithelial (A549), human histiocytic lymphoma (U937), mouse microglia (BV2), and African green monkey kidney (VERO) cells were cultured and maintained in Dulbecco's Modified Eagle's Medium (DMEM) supplemented with heat-inactivated 10% fetal bovine serum (Nactor). 100 ng/ml PMA (Sigma) was used to induce adherence of U937 cells. The JEV P3 strain (GenBank: U47032.1) was stored in our laboratory, while ZIKV H/PF/2013 strain (GenBank: KJ776791) and DENV type-2 strain

(GenBank: AF038403.1) were kindly provided by Dr. Bo Zhang, Wuhan Institute of Virology, Chinese Academy of Sciences. JEV was propagated in BHK cells, and DENV, ZIKV was propated in C6/36.

2.2 JEV infection and drug treatment

Artemisinin and artesunate (Selleck) were dissolved in DMSO at a concentration of 50 mM for storage and usage. Adult 6-week-old C57BL6J mice were randomly assigned to six groups, 15 each: DMSO; Artemisinin; Artesunate; JEV; JEV+Artemisinin; and JEV+Artesunate. Mice were intraperitoneally injected with 10^5 PFU of the JEV P3 strain in 200 μl DMEM (JEV, JEV+Artemisinin, and JEV+Artesunate groups) or 200 μl DMEM (DMSO, Artemisinin, and Artesunate groups) on day 0. Artemisinin (10 mg/kg body weight), artesunate (10 mg/kg body weight), or an equal volume of DMSO was intravenously administered in mice on day 3 and 4 post-infection. On day 5, five mice from each group were euthanized, and samples were collected for subsequent experiments. The remaining mice from each group were monitored daily to record behavioral signs and mortality. All animal experiments were performed according to the National Institutes of Health *Guide for the Care and Use of Laboratory Animals*, and the experimental protocols were approved by the Research Ethics Committee of the College of Veterinary Medicine, Huazhong Agricultural University, Hubei, Wuhan, China (HZAUMO-2018-012).

2.3 Cell viability assay

The viability of cultured cells was examined using the CellTiter-Glo® One Solution Assay kit (Promega) according to the manufacturer's instruction. After treatments, luminescence signals were recorded by a multimode plate reader.

2.4 Western Blotting

Equivalent amounts of proteins were separated by sodium dodecyl sulfate-polyacrylamide gel electrophoresis and electroblotted onto a polyvinylidene fluoride membrane (Millipore) using a Mini Trans-Blot Cell (Bio-Rad). Membranes were then blocked by incubating in the blocking buffer for 1h and probed with relevant antibodies. The blots were detected using the enhanced chemiluminescent (ECL) reagent (Thermo Fisher Scientific). Monoclonal antibodies against JEV E and NS5 proteins were prepared by our laboratory (Chen et al., 2012). Antibodies against IRF3, STAT1, p-STAT1-Y701, and p-STAT2-Y890 were purchased from ABclonal Technology. Anti-STAT2 and anti-p-IRF3-S386 antibodies were purchased from Cell Signaling Technology. Other antibodies used include anti-GAPDH antibody (Proteintech) and horseradish peroxidase-conjugated goat anti-mouse antibody (Boster).

2.5 Plaque assay

Cell supernatants were harvested, serially diluted, and then used to inoculate monolayers of VERO cells. After the removal of unbound viral particles, cells were incubated with DMEM containing 2% fetal bovine serum and 1.5% sodium carboxymethyl cellulose (Sigma) for 4 days. Subsequently, cells were fixed with 10% formaldehyde and stained with crystal violet solution to count visible plaques.

2.6 Quantitative reverse-transcription PCR (qRT-PCR)

Total cellular RNAs were extracted using TRIZOL Reagent (Invitrogen). The cDNA was synthesized by reverse transcription using a ReverTra Ace RT kit (Toyobo). qRT-PCR was performed using the QuantStudio 6 Flex PCR system (Applied Biosystems) and SYBR green PCR master mix (Toyobo). The results were normalized to the endogenous expression of β-actin in each sample. The primers are listed in Supplementary Table 1.

2.7 Hematoxylin and eosin (H&E) staining, immunohistochemistry (IHC) analysis, and terminal deoxynucleotidyl transferase-mediated dUTP nick end labelling (TUNEL) assay

All mice were anesthetized with ketamine-xylazine (0.1 ml per 10 g of body weight). Brain tissues were collected and embedded in paraffin for coronal sections. The sections were used for H&E staining, IHC, and TUNEL assay. For IHC, the primary antibodies were glial fibrillary acidic protein (GFAP, Servicebio), ionized calcium binding adapter molecule-1 (IBA-1, Servicebio), or neuronal nuclei (NeuN, Servicebio). For TUNEL assay, an In Situ Cell Death Detection Kit (Roche) was used according to the manufacturer's instructions (Huang et al., 2019).

2.8 Statistical analysis

All experiments were performed at least three times under similar conditions. Analyses were conducted using GraphPad Prism Software (version 7). Statistical differences among the experimental groups were determined using the two-way analysis of variance (ANOVA) with subsequent Student's test. *P*-value of <0.05 was considered significant.

3. Results

3.1 Artemisinin and artesunate reduce mouse lethality caused by JEV infection

Since artemisinin has previously been reported to show antiviral effects against several viruses (Liu et al., 2019), it is interesting to know whether it has a protective role against flavivirus infection. We chose a JEV-infected mouse model to examine the effect of artemisinin and artesunate (Figure 1a). A high mortality rate of 100% was observed in DMSO-treated mice challenged to JEV infection (Figure 1b). In contrast, treatment with artemisinin or artesunate protected the mice from JEV-caused lethality, with a survival rate of 50% and 60%, respectively (Figure 1b). Also, treatment with artemisinin or artesunate caused no significant

reduction in body weight (Figure 1c) and improved behavioral signs (Figure 1d) in JEV-infected mice. Furthermore, body organs collected on day 5 showed a marked decrease in viral load upon artemisinin or artesunate treatment when compared with non-treated infected mice (Figure 1e). No virus was detected in body organs of surviving mice collected on day 23 post-infection (Figure 1f). Overall, these results demonstrate that both artemisinin and artesunate protect mice from the JEV-induced lethality.

3.2 Artemisinin and artesunate abrogate JEV-induced inflammatory response in mouse brain tissues

Given the role of artemisinin and artesunate in reducing the JEV-induced mouse lethality, we asked whether these drugs abrogate the neuroinflammatory response triggered by JEV infection. Both drugs were found to completely inhibit the JEV replication in mice brain tissues as determined by Western blot analysis and plaque assay (Supplementary Figure 1a-b). As shown in Figure 2a, on day 5 post-infection, JEV infection induced a massive release of inflammatory cytokines, whereas the artemisinin or artesunate treatment significantly abolished the production of JEV-induced inflammatory cytokines. The histopathological analysis of mice brain tissues displayed characteristic features of acute encephalitis: meningitis and perivascular cuffing. However, artemisinin or artesunate treatment ameliorated JEV-infected encephalitis in mice (Figure 2b). An anomalous upsurge in the number of activated glia (astrocytes and microglia) and decrease in the number of neuronal cells were detected on day 5 post-infection, whereas artemisinin or artesunate treatment diminished the astrogliosis, microgliosis, and neuronal cell death in infected mice (Figure 2c–e and 2g). When compared with the JEV-infected mice, the number of TUNEL-positive cells were significantly reduced upon the treatment of infected mice with artemisinin or artesunate (Figure 2f–g). All surviving mice exhibited normal inflammatory cytokine levels and histological features at

23 days post-infection (Figure 2a–g). Taken together, these results showed that artemisinin and artesunate attenuated the neuroinflammatory response triggered by JEV infection.

3.3 Artemisinin inhibits the replication of flaviviruses *in vitro*

To determine whether artemisinin causes a direct antiviral effect against JEV and other mosquito-borne flaviviruses, a series of *in vitro* experiments were performed. First, we examined the effect of artemisinin on the viability of cultured A549 cells using a luminescence-based cell viability assay (Figure 3a). The highest non-toxic concentration of artemisinin (200 µM) was used for subsequent experiments. The treatment of infected cells with artemisinin reduced the production of infectious viral particles: ~100-fold at 24h and >10-fold at 36 and 48h post-infection (Figure 3b) as determined by plaque assay. Consistently, the viral RNA expression levels were also found to be decreased significantly upon artemisinin treatment at 24, 36, and 48hpi (Figure 3c). Furthermore, the immunofluorescence analysis revealed that artemisinin led to ~10, 40, and 20% reduction of the JEV-E protein expression at 24, 36, and 48hpi, respectively (Figure 3d–e), and the detected JEV-E protein fluorescence intensity was ~30% decreased at 36 and 48hpi as assessed by high content screening (Figure 3e). To determine the IC50 of artemisinin, the effect on the viral titers was examined upon the increasing concentration of the drug. Artemisinin inhibited the JEV particle production in a concentration-dependent manner (Figure 3f, left panel) with an IC50 of 18.5 µM (Figure 3f, right panel). To evaluate whether the artemisinin-induced anti-JEV effect is cell type-dependent or not, the effect of highest non-toxic concentration of artemisinin (Figure 3g) on JEV replication in cultured U937 (200 µM), BV2 (100 µM), and VERO (200 µM) cells was tested. The anti-JEV activity of artemisinin in U937 and BV2 cells was analogous to that as observed in A549 cells, whereas no antiviral effect was observed in VERO cells (Figure 3h–i). These results suggest a direct antiviral effect of artemisinin against

JEV. Since VERO is an interferon (IFN)-deficient cell line, we speculated that the artemisinin-induced antiviral effect might be associated with the type I IFN (IFN-I) response of the host.

We next evaluated the antiviral activity of artemisinin against other flaviviruses such as DENV and ZIKV. Akin to JEV, artemisinin significantly repressed the replication of DENV (Figure 4a–c) and ZIKV (Figure 4d–f) in A549 cells at 24, 36, and 48hpi, and in a drug-dose-dependent manner as determined by plaque assay and qRT-PCR. The IC50 of artemisinin for DENV and ZIKV was determined as 21.71 μM and 56.42 μM, respectively (Figure 4c and 4f, right panel). However, artemisinin caused no anti-DENV and anti-ZIKV activities in VERO cells (Figure 4g–j). These data suggest that artemisinin exerts broad-spectrum anti-flavivirus activity and that IFN-I response might be essential for the artemisinin-mediated antiviral activity.

3.4 Artemisinin exerts antiviral effect after virus entry into the host cells

To delineate the potential antiviral mechanism of artemisinin against flaviviruses, we examined whether artemisinin is impeding a pre- or post-entry phase of the virus life cycle. To this end, cultured A549 cells were subjected to three types of treatments: JEV infection followed by artemisinin treatment, artemisinin treatment followed by JEV infection, and co-administration of artemisinin and JEV particles. Treatment of artemisinin before and after JEV infection impaired the production of viral particles and the expression of viral proteins; however, these effects were found to be less significant upon co-administration of artemisinin with JEV (Figure 5a–b). Next, we examined the effect of artemisinin on the cellular adsorption and invasion phases of the viral life cycle. As shown in figure 5c and 5d, virus attachment to the cell surface and the subsequent cell entry process remained unchanged upon artemisinin treatment. These findings suggest that artemisinin does not disrupt the cell-binding and entry capability of the virus.

3.5 Artemisinin promotes IFN-I production and response after flavivirus infection

Considering our observation that IFN-I response might be related to the artemisinin-induced antiviral activity, we determined the impact of artemisinin on the production of IFN-I and the expression of downstream ISGs. Our data revealed that the treatment of JEV-infected A549 cells with artemisinin significantly promoted the mRNA expression and secretion of IFN-β (Figure 6a) and the transcription of ISGs (Figure 6b) when compared with the non-treated JEV-infected cells. The levels of IFN-β and ISGs were also found to be significantly increased upon artemisinin treatment of DENV (Figure 6c–d) or ZIKV (Figure 6e–f) infected A549 cells. Similar to A549 cells, artemisinin treatment promoted the IFN-β production in both U937 and BV2 cells after JEV infection (Figure 6g). Furthermore, significantly increased levels of IFN-β in blood and spleen samples of artemisinin or artesunate-treated mice were observed when compared with untreated mice during JEV infection (Supplement Figure 2a-b). Thus, these data indicate that artemisinin promotes a stronger IFN-I production and response upon flavivirus infection both *in vitro* and *in vivo*.

To further verify the conclusion, the activation of key signaling molecules associated with IFN-I was analyzed. Our results showed that JEV infection markedly increased the phosphorylation of IRF3, a key transcriptional factor of IFN-I (Jefferies, 2019), and STAT1 and STAT2, the signal transducers activated by IFN (Garcia-Diaz et al., 2019). The phosphorylation levels of these signaling molecules were further enhanced upon artemisinin treatment, whereas no obvious difference in their expression was observed (Supplement Figure 3a-b). These findings suggest that artemisinin treatment promotes the activation of both upstream and downstream signaling of IFN-I.

3.6 Artemisinin inhibits flavivirus infection through promoting the host IFN-I response

To further elucidate the artemisinin-induced anti-flavivirus activity through stimulation of the host IFN-I response, we used IFNAR polyclonal antibody (IFNAR pAb) to block the IFN-I pathway triggered by artemisinin treatment of infected cells. To this end, cultured cells were pre-incubated with IFNAR pAb followed by JEV infection and artemisinin treatment. It was observed that IFNAR pAb markedly inhibited the artemisinin-stimulated expression of interferon-stimulated genes (ISGs) in JEV-infected cells in a dose-dependent manner, whereas the control IgG had no effect on ISGs expression levels (Figure 7a). In addition, we also evaluated the effect of IFNAR blocking on the artemisinin-induced antiviral activity. Our data revealed that the incubation of cells with IFNAR pAb, but not with IgG, rescued the JEV replication halted by artemisinin, determined by plaque assay (Figure 7b) and qRT-PCR (Figure 7c). Hence, these findings suggest that the host IFN response plays a crucial role in mediating the artemisinin-induced antiviral activity.

4. Discussion

Previous studies have described artemisinin as an antiviral and a potential therapeutic agent for some RNA viruses (Lu et al., 2019; O'Flaherty et al., 2019). Considering this, we examined the effects of artemisinin and its derivative, artesunate, on viral replication and JEV-induced neuropathogenesis using a mouse model. It was observed that artemisinin or artesunate treatment inhibited viral replication in JEV-infected mice and abrogated the hallmark features of encephalitis in mouse brain tissues. These findings suggest that both artemisinin and artesunate exert therapeutic activity against JEV. This therapeutic activity might be mediated by the antiviral effects of artemisinin, since fewer viruses entering the brain would lead to lower neuroinflammatory response; conversely, the reduced viral load could be a beneficial result of attenuated inflammation. The direct anti-flaviviral activity of artemisinin was further verified by *in vitro* analysis of higher innate immune response, which could potentially

attenuate the progression of events leading to morbidity and mortality due to JEV infection, and thus, seems to be a novel remedy against Japanese encephalitis (Zheng et al., 2019). Artemisinin was reported to ameliorate inflammation via inflammatory-related signaling pathway (Long et al., 2016; Wu et al., 2016), but the protective effect of these drugs against Japanese encephalitis may engage other host processes that need to be investigated in future studies.

The antiviral mechanism of artemisinin and its derivative compounds is largely unknown. A previous study suggests that artesunate inhibits human cytomegalovirus replication by interfering with the NF-κB pathway (Flobinus et al., 2014). In our *in vitro* study, we discovered that artemisinin inhibits viral replication in A549, U937, and BV2 cells, but not in VERO cells, indicating the possible role of the host IFN in mediating the artemisinin-induced antiviral effects. Specifically, artemisinin was found to increase the levels of IFN-β and downstream ISGs in JEV-, DENV-, or ZIKV-infected cells. Similar findings were also observed in the spleen and blood samples of JEV-infected mice. The ISGs such as ISG56, MxA and OAS-1, are important downstream IFN pathway signaling molecules that exert a direct antiviral effect (Goodwin et al., 2019). Additionally, IRF3 is one of the most vital transcriptional factors of IFN-I: the activation of IRF3 is symbolized with the induction of IFN-I (Tsuchiya et al., 2019; Wei et al., 2019). Similarly, the phosphorylation of STAT1/STAT2 is widely recognized as a sign of activation of IFN-I signaling (Ramanan et al., 2011; Szelag et al., 2016). Here, the increased phosphorylation of IRF3 and STAT1/STAT2 implies that both upstream and downstream signaling pathways of IFN-I were stimulated by artemisinin. Moreover, the blocking of the IFN-I pathway using IFNAR antibodies rescued the JEV replication in infected cells. These findings suggest a novel IFN-mediated antiviral mechanism of artemisinin against flaviviruses. However, the precise molecular mechanism by which artemisinin induces the

expression of IFN remains unclear. The observed mechanism could be associated either with the overstimulation of innate immune signaling molecules or with the inhibitory effect on IFN-antagonizing strategies of flaviviruses. The possible involvement of these two hypothetical mechanisms requires further exploration.

5. Conclusion

In summary, our *in vitro* and *in vivo* study provides the first evidence that artemisinin inhibits the replication of flaviviruses by enhancing the host IFN-I response upon viral infection. The observed antiviral activity was found to be associated with reduced viremia, neuroinflammation, and mortality in JEV-infected mice. Therefore, artemisinin could be employed as a therapeutic option to inhibit the replication of multiple mosquito-borne flaviviruses and to halt neuroinflammation caused by neurotropic flaviviruses.

Acknowledgements

We thank Dr. Bo Zhang, Wuhan Institute of Virology, Chinese Academy of Sciences for kindly providing the ZIKV H/PF/2013 strain and the DENV type-2 strain.

Funding: This work was supported by National Key Research and Development Program of China (2016YFD0500407); National Natural Science Foundation of China (31825025 and 31972721); Fundamental Research Funds for the Central Universities (2662018QD025); and Natural Science Foundation of Hubei Province (2019CFA010).

Reference

Amorim, J.F.S., Azevedo, A.S., Costa, S.M., Trindade, G.F., Basílio-de-Oliveira, C.A., Gonçalves, A.J.S., Salomão, N.G., Rabelo, K., Amaral, R., Geraldo, L.H.M., Lima,

F.R.S., Mohana-Borges, R., Paes, M. V, Alves, A.M.B., 2019. Dengue infection in mice inoculated by the intracerebral route: neuropathological effects and identification of target cells for virus replication. Scientific Reports 9, 17926. https://doi.org/10.1038/s41598-019-54474-7

Ashraf, U., Zhu, B., Ye, J., Wan, S., Nie, Y., Chen, Z., Cu, M., Wang, C., Duan, X., Zhang, H., Chen, H., Cao*, S., 2016. MicroRNA-19b-3p Modulates Japanese Encephalitis Virus-Mediated Inflammation via Targeting RNF11. Journal of Virology 90, 4780–4795. https://doi.org/10.1128/jvi.02586-15

Boldescu, V., Behnam, M.A.M., Vasilakis, N., Klein, C.D., 2017. Broad-spectrum agents for flaviviral infections: Dengue, Zika and beyond. Nature Reviews Drug Discovery 16, 565–586. https://doi.org/10.1038/nrd.2017.33

Bradley J. Blitvich, and A.E.F., 2017. A review of flaviviruses that have no known arthropod vector. Viruses 9, 1–25. https://doi.org/10.3390/v9060154

Calderón-Peláez, M.A., Velandia-Romero, M.L., Bastidas-Legarda, L.Y., Beltrán, E.O., Camacho-Ortega, S.J., Castellanos, J.E., 2019. Dengue virus infection of blood-brain barrier cells: Consequences of severe disease. Frontiers in Microbiology 10, 1435. https://doi.org/10.3389/fmicb.2019.01435

Capasso, A., Ompad, D.C., Vieira, D.L., Wilder-Smith, A., Tozan, Y., 2019. Incidence of Guillain-Barré Syndrome (GBS) in Latin America and the Caribbean before and during the 2015-2016 Zika virus epidemic: A systematic review and meta-analysis. PLoS Neglected Tropical Disease. 13, e0007622. https://doi.org/10.1371/journal.pntd.0007622

Carlo Amorin Daep·Jorge L. Muñoz-Jordán·Eliseo Albɛrto Eugenin, 2014. Flaviviruses, an expanding threat in public health: focus on dengue, West Nile, and Japanese encephalitis

virus. Journal of NeuroVirology 20, 539–560. https://doi.org/10.1007/s13365-014-0285-z

Chen, Z., Shao, L., Ye, J., Li, Y., Huang, S., Chen, H., Cao, S., 2012. Monoclonal antibodies against NS3 and NS5 proteins of Japanese encephalitis virus. Hybridoma 31, 137–41. https://doi.org/10.1089/hyb.2011.0107

Chen, Z., Wang, X., Ashraf, U., Zheng, B., Ye, J., Zhou, D., Zhang, H., Song, Y., Chen, H., Zhao, S., Cao, S., 2018. Activation of neuronal N-methyl-d-aspartate receptor plays a pivotal role in Japanese encephalitis virus-induced neuronal cell damage. Journal of Neuroinflammation 15, 238. https://doi.org/10.1186/s12974-018-1280-8

Denny, J.E., Schmidt, N.W., Mu, X., Wang, C., 2019. Oral Administration of Clinically Relevant Antimalarial Drugs Does Not Modify the Murine Gut Microbiota. Scientific Reports 9, 11952. https://doi.org/10.1038/s41598-019-48454-0

Diamond, M.S., 2003. Evasion of innate and adaptive immunity by flaviviruses. Immunology and Cell Biology. https://doi.org/10.1046/j.1440-1711.2003.01157.x

E A Gould, T.S., 2008. Pathogenic flaviviruses. Lancet 371, 500–9. https://doi.org/10.1016/S0140-6736(08)60238-X

Efferth, T., 2018. Beyond malaria: The inhibition of viruses by artemisinin-type compounds. Biotechnology Advances 36, 1730–1737. https://doi.org/10.1016/j.biotechadv.2018.01.001

Efferth, T., Romero, M.R., Wolf, D.G., Stamminger, T., Marin, J.J.G., Marschall, M., 2008. The Antiviral Activities of Artemisinin and Artesunate. Clinical Infectious Diseases 47, 804–11. https://doi.org/10.1086/591195

Flobinus, A., Taudon, N., Desbordes, M., Labrosse, B., Simon, F., Mazeron, M.C., Schnepf, N., 2014. Stability and antiviral activity against human cytomegalovirus of artemisinin

derivatives. Journal of Antimicrobial Chemotherapy 69, 34–40. https://doi.org/10.1093/jac/dkt346

Garcia-Diaz, A., Shin, D.S., Moreno, B.H., Saco, J., Escuin-Ordinas, H., Rodriguez, G.A., Zaretsky, J.M., Sun, L., Hugo, W., Wang, X., Parisi, G., Saus, C.P., Torrejon, D.Y., Graeber, T.G., Comin-Anduix, B., Hu-Lieskovan, S., Damoiseaux, R., Lo, R.S., Ribas, A., 2019. Interferon Receptor Signaling Pathways Regulating PD-L1 and PD-L2 Expression. Cell Reports 29, 3766. https://doi.org/10.1016/j.celrep.2019.11.113

Goodwin, C.M., Schafer, X., Munger, J., 2019. UL26 attenuates IKKβ-mediated induction of ISG expression and enhanced protein ISGylation during HCMV infection. Journal of Virology 93, e01052-19. https://doi.org/10.1128/jvi.01052-19

Gregorius J. Sips, Jan Wilschut, J.M.S., 2012. Neuroinvasive flavivirus infections. Reviews in Medical Virology 22, 69–87. https://doi.org/10.1002/rmv.712

Hirsch, A.J., Roberts, V.H.J., Grigsby, P.L., Haese, N., Schabel, M.C., Wang, X., Lo, J.O., Liu, Z., Kroenke, C.D., Smith, J.L., Kelleher, M., Broeckel, R., Kreklywich, C.N., Parkins, C.J., Denton, M., Smith, P., DeFilippis, V., Messer, W., Nelson, J.A., Hennebold, J.D., Grafe, M., Colgin, L., Lewis, A., Ducore, R., Swanson, T., Legasse, A.W., Axthelm, M.K., MacAllister, R., Moses, A. V., Morgan, T.K., Frias, A.E., Streblow, D.N., 2018. Zika virus infection in pregnant rhesus macaques causes placental dysfunction and immunopathology. Nature Communications 9, 263. https://doi.org/10.1038/s41467-017-02499-9

Huang, S., Gu, J., Ye, J., Fang, B., Wan, S., Wang, C., Ashraf, U., Li, Q., Wang, X., Shao, L., Song, Y., Zheng, X., Cao, F., Cao, S., 2019. Benzoxazine monomer derived carbon dots as a broad-spectrum agent to block viral infectivity. Journal of Colloid and Interface Science 542, 198–206. https://doi.org/10.1016/j.jcis.2019.02.010

Idowu, A.O., Bhattacharyya, S., Gradus, S., Oyibo, W., George, Z., Black, C., Igietseme, J., Azenabor, A.A., 2018. Plasmodium falciparum treated with artemisinin-based combined therapy exhibits enhanced mutation, heightened cortisol and TNF-α induction. International Journal of Medical Sciences 15, 1449–1457. https://doi.org/10.7150/ijms.27350

Imran, Saleemi, Chen, Wang, Zhou, Li, Zhao, Zheng, Li, Cao, Ye, 2019. Decanoyl-Arg-Val-Lys-Arg-Chloromethylketone: An Antiviral Compound That Acts against Flaviviruses through the Inhibition of Furin-Mediated prM Cleavage. Viruses 11, 1011. https://doi.org/10.3390/v11111011

Jefferies, C.A., 2019. Regulating IRFs in IFN Driven Disease. Frontiers in Immunology 10, 325. https://doi.org/10.3389/fimmu.2019.00325

Liu, X., Lu, J., Liao, Y., Liu, S., Chen, Y., He, R., Men, L., Lu, C., Chen, Z., Li, S., Xiong, G., Yang, S., 2019. Dihydroartemisinin attenuates lipopolysaccharide-induced acute kidney injury by inhibiting inflammation and oxidative stress. Biomedicine and Pharmacotherapy 117, 109070. https://doi.org/10.1016/j.biopha.2019.109070

Long, H., Xu, B., Luo, Y., Luo, K., 2016. Artemisinin protects mice against burn sepsis through inhibiting NLRP3 inflammasome activation. American Journal of Emergency Medicine 34, 772–7. https://doi.org/10.1016/j.ajem.2015.12.075

Lu, B.W., Baum, L., So, K.F., Chiu, K., Xie, L.K., 2019. More than anti-malarial agents: Therapeutic potential of artemisinins in neurodegeneration. Neural Regeneration Research 14, 1494–1498. https://doi.org/10.4103/1673-5374.255960

Maximova, O.A., Pletnev, A.G., 2018. Flaviviruses and the Central Nervous System: Revisiting Neuropathological Concepts. Annual Review of Virology 5, 255–272. https://doi.org/10.1146/annurev-virology-092917-043439

Mustafá, Y.M., Meuren, L.M., Coelho, S.V.A., de Arruda, L.B., 2019. Pathways Exploited by Flaviviruses to Counteract the Blood-Brain Barrier and Invade the Central Nervous System. Frontiers in Microbiology 10, 525. https://doi.org/10.3389/fmicb.2019.00525

Ngono, A.E., Shresta, S., 2018. Immune Response to Dengue and Zika. Annual Review of Immunology 36, 279–308. https://doi.org/10.1146/annurev-immunol-042617-053142

O'Flaherty, K., Ataíde, R., Zaloumis, S.G., Ashley, E.A., Powell, R., Feng, G., Reiling, L., Dondorp, A.M., Day, N.P., Dhorda, M., Fairhurst, R.M., Lim, P., Amaratunga, C., Pukrittayakamee, S., Hien, T.T., Htut, Y., Mayxay, M., Faiz, M.A., Beeson, J.G., Nosten, F., Simpson, J.A., White, N.J., Fowkes, F.J.I., 2019. Contribution of Functional Antimalarial Immunity to Measures of Parasite Clearance in Therapeutic Efficacy Studies of Artemisinin Derivatives. Journal of Infectious Diseases 220, 1178–1187. https://doi.org/10.1093/infdis/jiz247

Olagnier, D., Muscolini, M., Coyne, C.B., Diamond, M.S., Hiscott, J., 2016. Mechanisms of Zika Virus Infection and Neuropathogenesis. DNA and Cell Biology 35, 367–72. https://doi.org/10.1089/dna.2016.3404

Ramanan, P., Shabman, R.S., Brown, C.S., Amarasinghe, G.K., Basler, C.F., Leung, D.W., 2011. Filoviral Immune Evasion Mechanisms. Viruses 3, 1634–49. https://doi.org/10.3390/v3091634

Sharma, B.N., Marschall, M., Rinaldo, C.H., 2014. Antiviral effects of artesunate on JC polyomavirus replication in COS-7 Cells. Antimicrobial Agents and Chemotherapy 58, 6724–6734. https://doi.org/10.1128/AAC.03714-14

Szelag, M., Piaszyk-Borychowska, A., Plens-Galaska, M., Wesoly, J., Bluyssen, H.A.R., 2016. Targeted inhibition of STATs and IRFs as a potential treatment strategy in cardiovascular disease. Oncotarget 7, 48788–48812. https://doi.org/10.18632/oncotarget.9195

Tsuchiya, N., Zhang, R., Iwama, T., Ueda, N., Liu, T., Tatsumi, M., Sasaki, Y., Shimoda, R., Osako, Y., Sawada, Y., Kubo, Y., Miyashita, A., Fukushima, S., Cheng, Z., Nakaki, R., Takubo, K., Okada, S., Kaneko, S., Ihn, H., Kaisho, T., Nishimura, Y., Senju, S., Endo, I., Nakatsura, T., Uemura, Y., 2019. Type I Interferon Delivery by iPSC-Derived Myeloid Cells Elicits Antitumor Immunity via XCR1+ Dendritic Cells. Cell Reports 29, 162-175.e9. https://doi.org/10.1016/j.celrep.2019.08.086

Wei, F., Jiang, Z., Sun, H., Pu, J., Sun, Y., Wang, M., Tong, Q., Bi, Y., Ma, X., Gao, G.F., Liu, J., 2019. Induction of PGRN by influenza virus inhibits the antiviral immune responses through downregulation of type I interferons signaling. PLOS Pathogens 15, e1008062. https://doi.org/10.1371/journal.ppat.1008062

Wohlfarth, C., Efferth, T., 2009. Natural products as promising drug candidates for the treatment of hepatitis B and C. Acta Pharmacologica Sinica. https://doi.org/10.1038/aps.2008.5

Wong, Y.K., Xu, C., Kalesh, K.A., He, Y., Lin, Q., Wong, W.S.F., Shen, H.M., Wang, J., 2017. Artemisinin as an anticancer drug: Recent advances in target profiling and mechanisms of action. Medicinal Research Reviews 37, 1492–1517. https://doi.org/10.1002/med.21446

Wu, Y., He, S., Bai, B., Zhang, L., Xue, L., Lin, Z., Yang, X., Zhu, F., He, P., Tang, W., Zuo, J., 2016. Therapeutic effects of the artemisinin analog SM934 on lupus-prone MRL/lpr mice via inhibition of TLR-triggered B-cell activation and plasma cell formation. Cellular and Molecular Immunology 13, 379–90. https://doi.org/10.1038/cmi.2015.13

Ye, J., Zhu, B., Fu, Z.F., Chen, H., Cao, S., 2013. Immune evasion strategies of flaviviruses. Vaccine. https://doi.org/10.1016/j.vaccine.2012.11.015

Zhang, H., Sun, J., Ye, J., Ashraf, U., Chen, Z., Zhu, B., He, W., Xu, Q., Wei, Y., Chen, H., Fu, Z.F., Liu, R., Cao, S., 2015. Quantitative Label-Free Phosphoproteomics Reveals

Differentially Regulated Protein Phosphorylation Involved in West Nile Virus-Induced Host Inflammatory Response. Journal of Proteome Research 14, 5157–68. https://doi.org/10.1021/acs.jproteome.5b00424

Zheng, B., Wang, X., Liu, Y., Li, Y., Long, S., Gu, C., Ye, J., Xie, S., Cao, S., 2019. Japanese Encephalitis Virus infection induces inflammation of swine testis through RIG-I—NF-κB signaling pathway. Veterinary Microbiology 238, 108430. https://doi.org/10.1016/j.vetmic.2019.108430

Figure Legends

Figure 1: Artemisinin and artesunate reduce mouse lethality induced by JEV infection. **(a)** Schematic of *in vivo* experimental model. Mice were intraperitoneally injected with 10^5 PFU of the JEV P3 strain in 200 μl DMEM or 200 μl DMEM on day 0. Artemisinin (10 mg/kg body weight), artesunate (10 mg/kg body weight), or an equal volume of DMSO was intravenously administered in mice on day 3 and 4 post-infection. Mice were euthanized, and samples were collected for subsequent experiments on day 5 and 23 post-infection. **(b–d)** Survival rate (b), body weight (c), and behavioral score (d) of mice in each experimental group were monitored for 23 days after JEV infection. Survival rate is shown as Kaplan-Meier survival curves. The behavioral score from 0 to 5 represents the mice behavioral changes from normal to severe. n = 10 mice. **(e and f)** Detection of viral loads in the mice body organs, collected on day 5 (e) and 23 (f) after JEV infection, by qRT-PCR. Figures are representative of five mice with similar results. *P < 0.05, ****P < 0.0001.

Figure 2: Artemisinin and artesunate reduce the JEV-induced neuroinflammatory response *in vivo*. (a) The mRNA expression levels of inflammatory cytokines (TNF-α, CCL-2, CCL-5, IL6, and IL-1β) in brain tissue lysates were quantified by qRT-PCR. **(b–e)** H&E

staining (b) and IHC (c–e) of mice brain tissues were performed to observe the pathological changes (b), astrogliosis (c), microgliosis (d), and neuronal cell death (e). Scale bar = 50 μm. **(f)** Neuronal apoptosis (green) was detected by the TUNEL assay. Scale bar = 200 μm. **(g)** The quantification of GFAP, IBA-1, and TUNEL positive cells in mice brain detected in figure c, d, and f, respectively. Figures are representative of five mice with similar results. ****P < 0.0001.

Figure 3: Artemisinin inhibits JEV replication *in vitro*. (a) Cell viability assay at indicated concentrations of artemisinin in A549 cells. **(b–d)** Effect of artemisinin on JEV replication. A549 cells were infected with JEV at MOI of 1. After 1h incubation, cells were washed and treated with 200 μM artemisinin. Viral titers (b), viral RNA levels (c), and viral E protein expression (d) at indicated time points were measured by plaque assay, qRT-PCR, and immunofluorescence analysis, respectively. Scale bar = 50 μm. **(e)** The quantification of JEV positive cells and fluorescence intensity in figure d was detected by high content screening instrument. **(f)** A549 cells were infected with 1MOI of JEV followed by treatment with indicated concentration of artemisinin. The viral titers in the medium were determined by plaque assay at 24h post-infection (left panel), and IC50 was calculated (right panel). **(g)** Cell viability assay at indicated concentrations of artemisinin in U937, BV2, and VERO cells. **(h and i)** U937, BV2, or VERO cells were infected with JEV at MOI of 1, followed by treatment with 200 μM artemisinin. Viral titers (h) and viral RNA levels (i) at indicated time points were measured by plaque assay and qRT-PCR, respectively. Data are expressed as means ± SEM from three independent experiments. *P < 0.05, **P < 0.01, ***P < 0.001, ****P < 0.0001.

Figure 4: Artemisinin inhibits the replication of DENV and ZIKV *in vitro*. A549 **(a–f)** or VERO **(g–j)** cells were infected at MOI of 5 with either DENV or ZIKV. Subsequently, infected cells were treated with artemisinin (200 μM) for a period of 48h. DENV (a and g) or

ZIKV (d and i) titers and DENV (b and h) or ZIKV (e and j) mRNAs levels at indicated time points were quantified by plaque assay and qRT-PCR, respectively. **(c)** A549 cells were infected with 5 MOI of DENV followed by treatment with indicated concentration of artemisinin. The viral titer in the medium was determined by focus forming assay at 24h post-infection (left panel), and IC50 was calculated (right panel). **(f)** A549 cells were infected with 5 MOI of ZIKV followed by treatment with indicated concentration of artemisinin. The viral titer in the medium was determined by plaque assay at 24h post-infection (left panel), and IC50 was calculated (right panel). Data are expressed as means ± SEM from three independent experiments. $^{**}P < 0.01$, ***P < 0.001, $^{****}P < 0.0001$.

Figure 5: Artemisinin exerts antiviral effect after virus entry into the host cells. (a and b) Drug treatment was performed in three different ways as follows. 1) JEV→Artemisinin: A549 cells were infected with 1 MOI JEV. After incubation at 37°C for 1h, cells were washed with DMEM, and then treated with 200 μM artemisinin. 2) Artemisinin→JEV: A549 cells were incubated with 200 μM artemisinin at 37°C for 2h. After washing with DMEM, cells were infected with 1 MOI JEV. After 1 h, cells were washed and incubated with fresh medium. 3) Artemisinin+JEV→: 1 MOI JEV and artemisinin (200 μM) were mixed and incubated at 37° C for 1h. The mixture was added to A549 cells followed by incubation at 37°C for 1h. Cells were then washed with DMEM and incubated with fresh medium. Samples were collected and subjected to subsequent experiments at 24hpi. Viral titers and the expression of JEV NS5 and E proteins were determined by plaque assay (a) and Western blot analysis (b), respectively. **(c)** A549 cells were treated with artemisinin and incubated at 37°C for 2h, and then cells were infected with 1 MOI JEV. After incubation at 4°C for 1h, cells were washed and samples were harvested to detect the expression of viral RNAs by qRT-PCR. **(d)** A549 cells were treated with artemisinin and incubated at 37°C for 2h, followed by 1 MOI JEV infection

and incubation for 1h at 4°C. Cells were then washed and incubated at 37°C for another 1h. Samples were collected to detect the expression of viral RNAs by qRT-PCR. Data are expressed as means ± SEM from three independent experiments. *$P < 0.05$, ****$P < 0.0001$.

Figure 6: Artemisinin promotes host IFN-I response after flavivirus infection. (a–f) A549 cells were infected with JEV (1 MOI), DENV (5 MOI), or ZIKV (5 MOI), followed by artemisinin treatment (200 μM). The mRNA levels of IFN-β, MxA, ISG56, and OAS-1 were measured by qRT-PCR. The secretion of IFN-β was detected by ELISA. **(g)** U937 or BV2 cells were treated with artemisinin (U937: 200 μM, BV2: 100μM) following JEV infection at 1 MOI. The IFN-β mRNA expression and secretion was tested by qRT-PCR and ELISA, respectively. Data are expressed as means ± SEM from three independent experiments. *$P < 0.05$, **$P < 0.01$, ***P < 0.001, ****$P < 0.0001$.

Figure 7: Artemisinin halts flavivirus infection through promoting the host type I IFN response. A549 cells were pre-incubated with IFNAR pAb at the indicated concentrations followed by JEV infection (1 MOI) and artemisinin treatment (200 μM) for 24h. **(a)** The mRNA expression levels of ISG56, MxA, and OAS-1 were measured by qRT-PCR. **(b and c)** Viral titers (b) and mRNA levels (c) were determined by plaque assay and qRT-PCR, respectively. Data are expressed as means ± SEM from three independent experiments. *$P < 0.05$, **$P < 0.01$, ***P < 0.001, ****$P < 0.0001$.

Supplementary Figure 1: Artemisinin and artesunate reduce JEV replication in mouse brain tissues. Mice were subjected to JEV infection and artemisinin or artesunate treatment as described in figure 1a. Brain samples were collected on day 5 and 23 post-infection. **(a)** The expression levels of JEV NS5 and E proteins were examined by Western blot. **(b)** Viral titers were determined by plaque assay. $n = 5$ mice. ****$P \leq 0.0001$.

Supplementary Figure 2: Artemisinin and artesunate enhance the IFN-β expression in blood and spleen of JEV-infected mice. Mice were subjected to JEV infection and artemisinin or artesunate treatment as described in figure 1a. The blood and spleen samples were collected on day 5 post-infection. **(a)** IFN-β mRNA expression in blood and spleen of mice was determined by qRT-PCR. **(b)** IFN-β production in blood and spleen of mice was measured by ELISA. $n = 5$ mice. *$P < 0.05$, **$P < 0.01$, ***P < 0.001, ****$P \leq 0.0001$.

Supplementary Figure 3: Artemisinin promotes the activation of IFN-I pathway-associated signaling molecules. (a) A549, U937, or BV2 cells were infected with 1 MOI JEV followed by treatment with artemisinin (200μM). Cells were collected at 24hpi and subjected to Western blot analysis by using indicated antibodies. **(b)** The protein levels were quantified by immunoblot scanning and normalized to the amount of GAPDH. Data are expressed as means ± SEM from three independent experiments. *$P < 0.05$, **$P < 0.01$, ***$P < 0.001$.

Figure 1

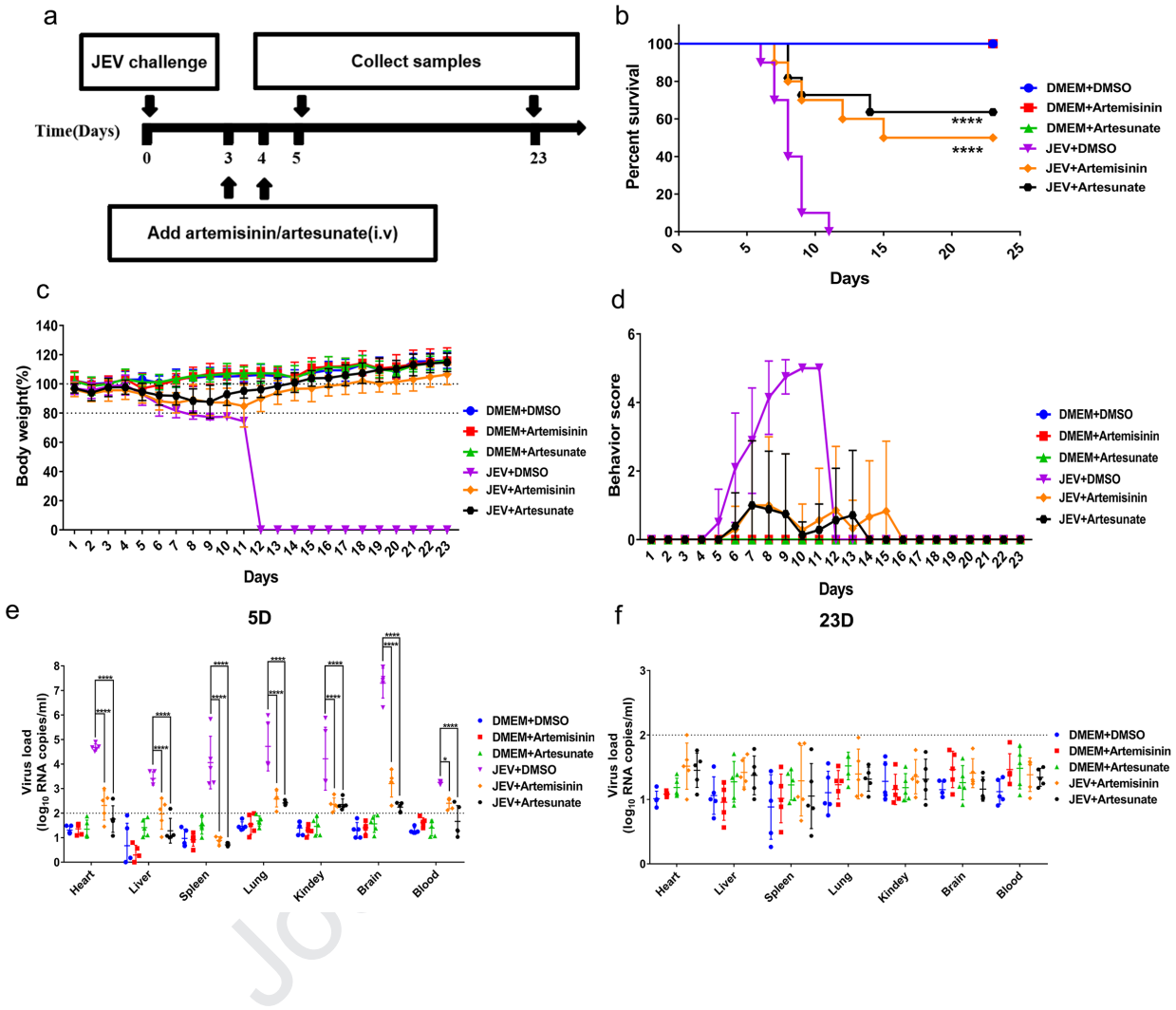
a
JEV challenge
Collect samples
Time(Days)
0
3
4
5
23
Add artemisinin/artesunate(i.v)
b
Percent survival
Days
****
****
DMEM+DMSO
DMEM+Artemisinin
DMEM+Artesunate
JEV+DMSO
JEV+Artemisinin
JEV+Artesunate
c
Body weight(%)
Days
d
Behavior score
Days
e
5D
Virus load (log10 RNA copies/ml)
Heart
Liver
Spleen
Lung
Kindey
Brain
Blood
f
23D
Virus load (log10 RNA copies/ml)

Figure 2

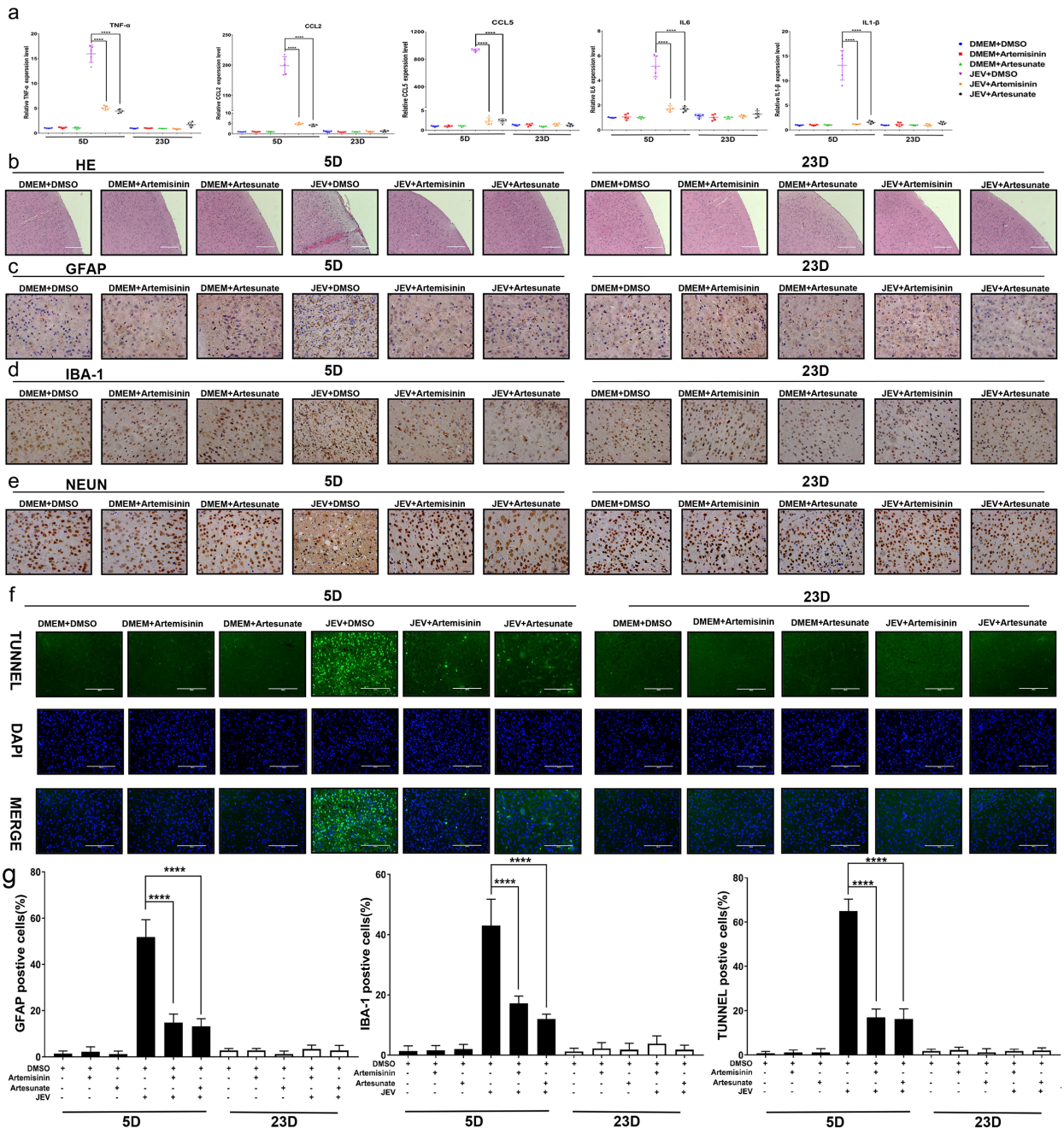
a
TNF-α
CCL2
CCL5
IL6
IL1-β
Relative TNF-α expression level
Relative CCL2 expression level
Relative CCL5 expression level
Relative IL6 expression level
Relative IL1-β expression level
5D
23D
DMEM+DMSO
DMEM+Artemisinin
DMEM+Artesunate
JEV+DMSO
JEV+Artemisinin
JEV+Artesunate
b HE
c GFAP
d IBA-1
e NEUN
f
TUNNEL
DAPI
MERGE
g
GFAP postive cells(%)
IBA-1 postive cells(%)
TUNNEL postive cells(%)
DMSO
Artemisinin
Artesunate
JEV
****

Figure 3

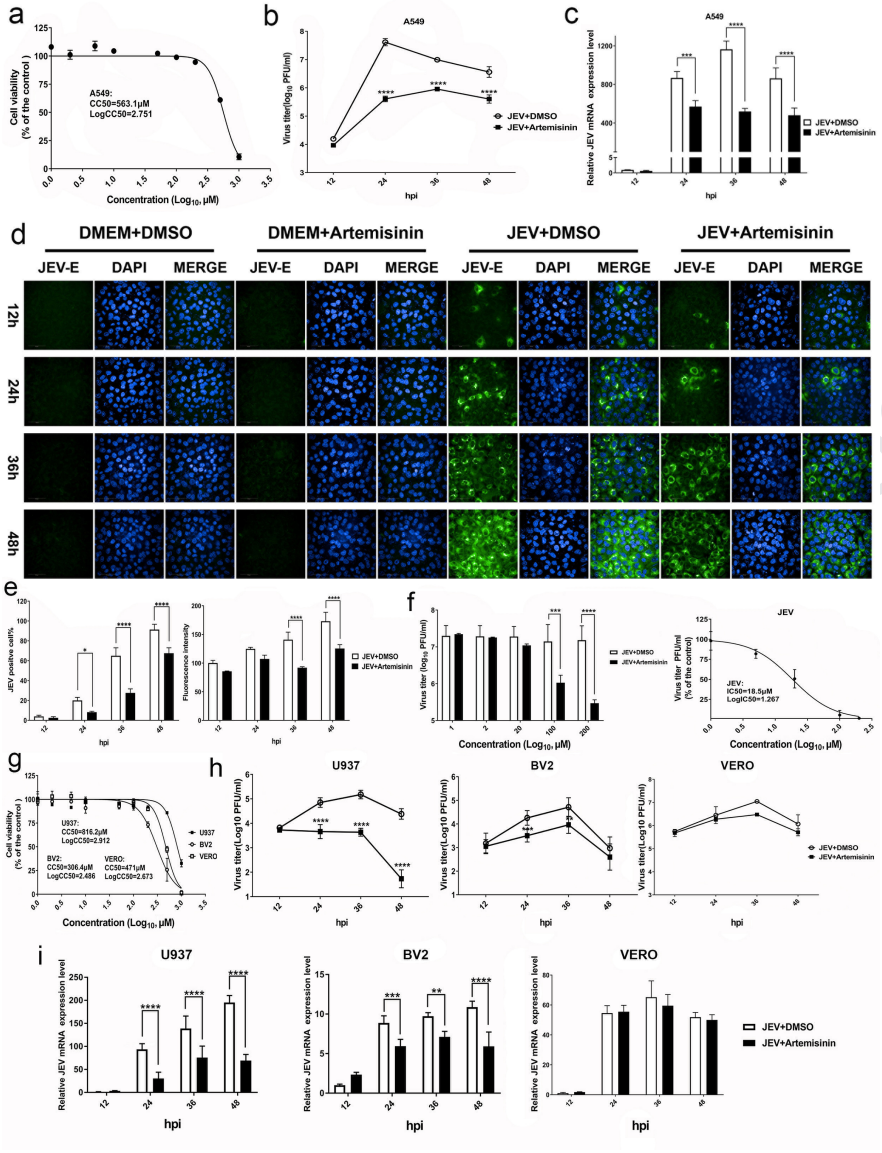
a
Cell viability (% of the control)
A549:
CC50=563.1μM
LogCC50=2.751
Concentration (Log10, μM)
b
A549
Virus titer(log10 PFU/ml)
JEV+DMSO
JEV+Artemisinin
hpi
c
A549
Relative JEV mRNA expression level
JEV+DMSO
JEV+Artemisinin
hpi
d
DMEM+DMSO
DMEM+Artemisinin
JEV+DMSO
JEV+Artemisinin
JEV-E
DAPI
MERGE
12h
24h
36h
48h
e
JEV positive cell%
Fluorescence intensity
JEV+DMSO
JEV+Artemisinin
hpi
f
Virus titer log10 PFU/ml
JEV+DMSO
JEV+Artemisinin
Concentration (Log10, μM)
JEV
Virus titer PFU/ml (% of the control)
JEV:
IC50=18.5μM
LogIC50=1.267
Concentration (Log10, μM)
g
Cell viability (% of the control)
U937:
CC50=816.2μM
LogCC50=2.912
BV2:
CC50=306.4μM
LogCC50=2.486
VERO:
CC50=471μM
LogCC50=2.673
U937
BV2
VERO
Concentration (Log10, μM)
h
U937
BV2
VERO
Virus titer(Log10 PFU/ml)
hpi
JEV+DMSO
JEV+Artemisinin
i
U937
BV2
VERO
Relative JEV mRNA expression level
hpi
JEV+DMSO
JEV+Artemisinin

Figure 4

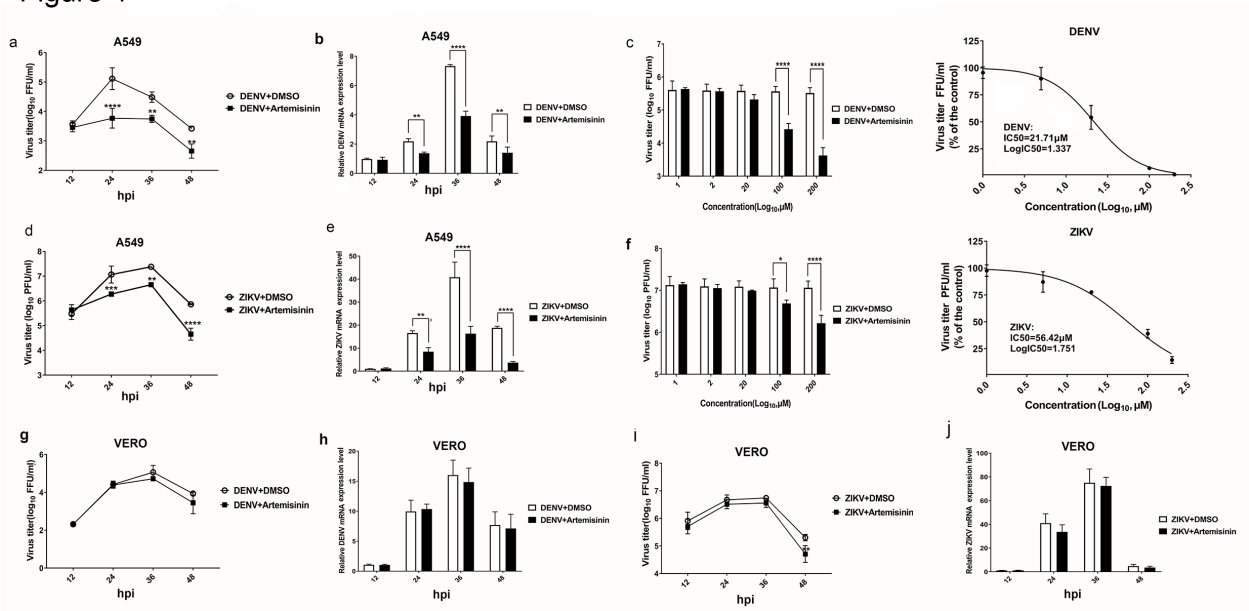

Figure 5

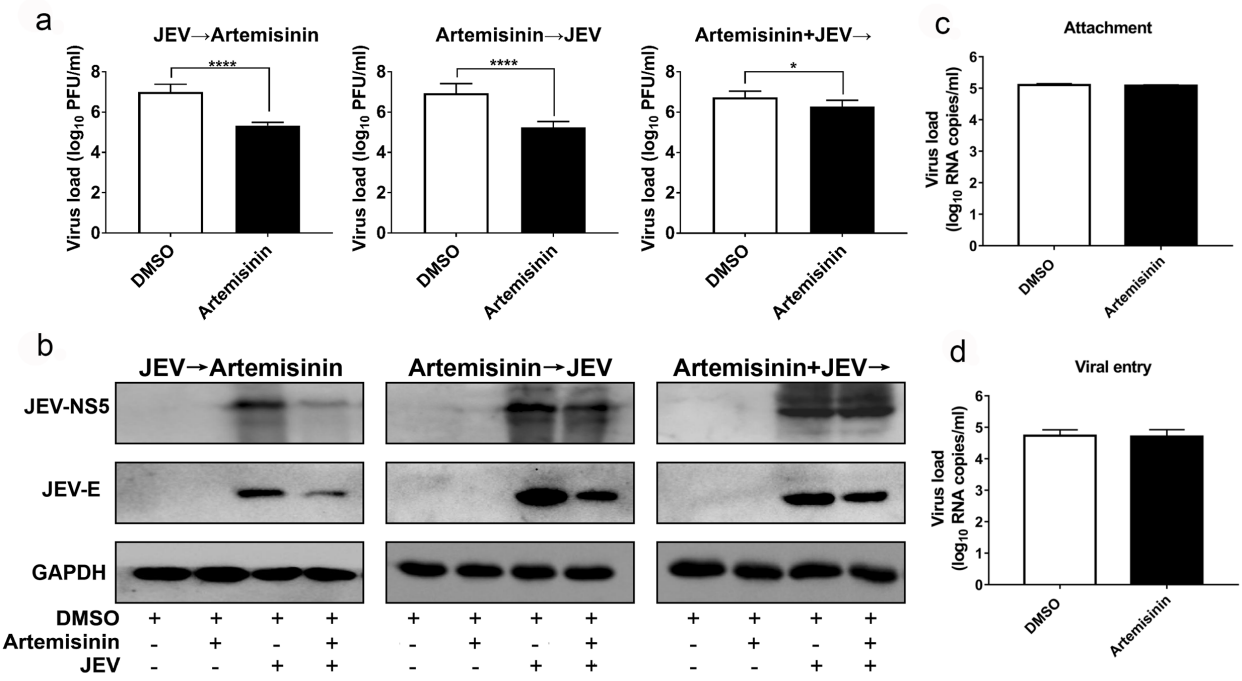

Figure 6

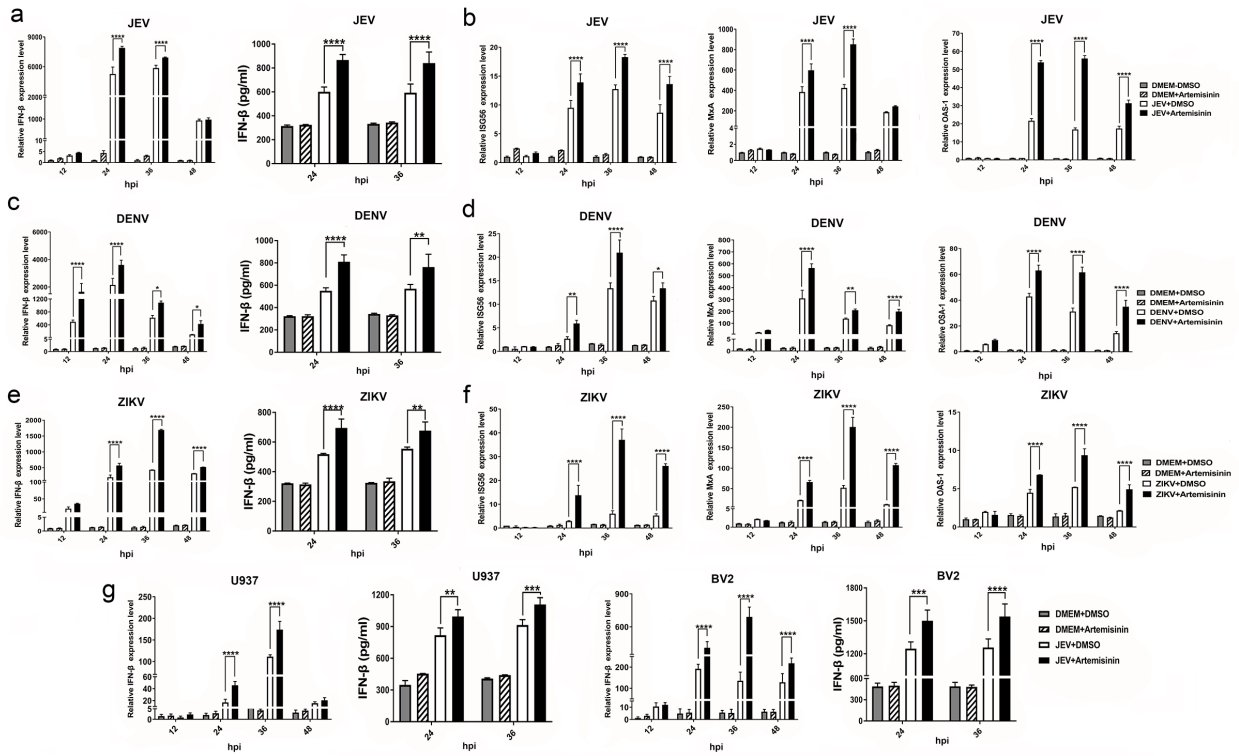

Figure 7

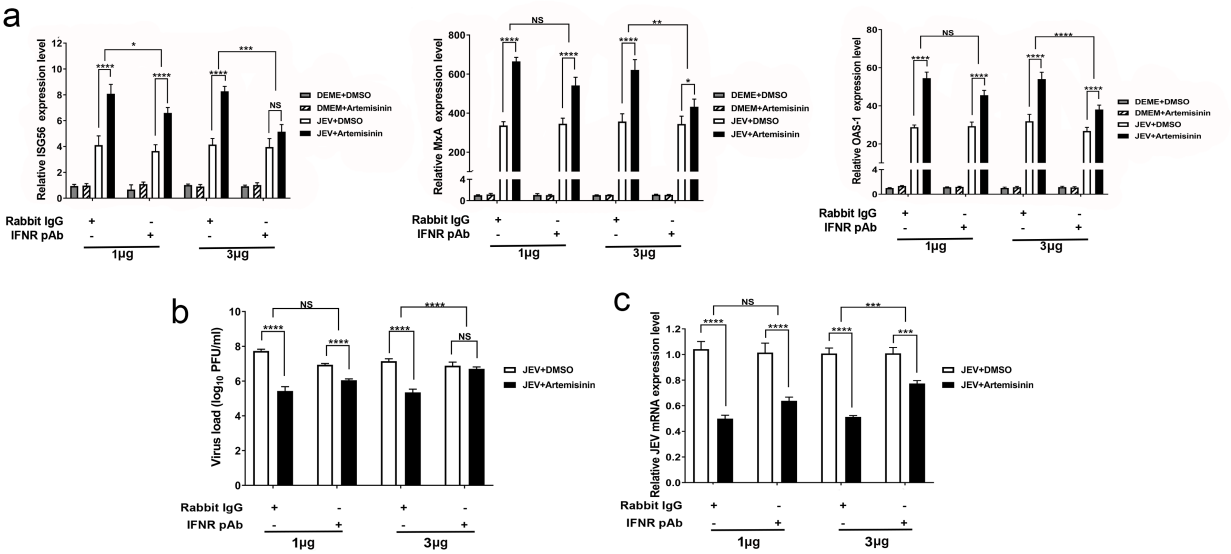

Highlights:

1. Artemisinin reduces lethality and brain damage in JEV-infected mice.
2. Artemisinin inhibits flavivirus replication both *in vitro* and *in vivo*.
3. Artemisinin inhibits flaviviruses' replication by promoting the host type I interferon production.